XLI CILAMCE
XLI Ibero-Latin American Congress on Computational Methods in Engineering
16-19 November, 2020 FOZ DO IGUAÇU PARANÁ - BRAZIL

A Nonlinear Boundary Element Coupling formulation for three-dimensional bond-slip analysis

Antonio R. Neto[1], Edson D. Leonel[1]

[1]*Department of Structural Engineering, São Carlos School of Engineering, University of São Paulo*
Av. Trabalhador SaoCarlense,400 , CEP 13566-590, São Carlos-SP, Brazil
anotonio.rodrigues.neto@usp.br, edleonel@sc.usp.br

Abstract. This study presents a numerical coupling formulation for the bond-slip modelling of 3D reinforced domains. This formulation is based on the Lagrangian 3D Boundary Element Method (BEM) and the 1DBEM/BEM coupling. In this technique, the material matrix (solid 3D domain) is represented by the 3D BEM displacements integral equation. Numerical integration and singularity subtraction are implemented for plane elements. A one-dimensional approach of the BEM (1DBEM) represents the embedded reinforcing bars. The 1DBEM is based on the axial fundamental solution for elastic 1D domains, which can be easily found in the literature. The interaction between the matrix and reinforcements is described by an adherence force over the reinforcements' line, which is interpolated by high-order polynomial functions. The adherence force is accounted as a body force into the 3D BEM formulation. The bond-slip effects are accounted by considering relative displacements between reinforcement and matrix. An adherence law represents the relation between slip and adherence force. Thus, Newton-Raphson solution technique can be utilised to solve the nonlinear problem. The boundary formulation is applied herein to represent the pullout test, which is essentially 3D. In this regard, a connection element is used to properly enforce the prescribed displacement directly at the reinforcing bar in a region outside the 3D solid. The numerical results of the pullout test model show excellent agreement with experimental data. Therefore, the proposed formulation can be considered stable, accurate and robust.

Keywords: Coupled BEM formulation, Reinforced materials, 3D BEM, Bond-slip

1 Introduction

The use of reinforced materials and structures in complex engineering components has grown considerably recently. With that, one can achieve efficient designs with these compositions, i.e., high high stiffness and low weight. Hence, its accurate mechanical modelling becomes absolutely necessary. In this context, the coupling of dissimilar numerical methods is widely applied and the FEM/BEM (Finite Element Method/Boundary Element Method) coupling proposed by Zienkiewicz et al. [1] stands out. Rodrigues Neto and Leonel [2] proposed an alternative coupling based only in BEM formulations, named 1DBEM/BEM, for 2D analyses. In this coupling technique, the 3D BEM represents the solid matrix and a 1D approach of the BEM model the reinforcing fibres. Besides, a nonlinear formulation was presented regarding the fibres elastoplasticity.

This study presents extension of the 1DBEM/BEM coupling formulation for 3D analyses. Furthermore, the adherence loss phenomenon is considered herein. Thus, a nonlinear bond-slip formulation is developed. BEM formulations have already been applied for 2D bond-slip analyses in the literature, as one can find in Rocha et al. [3]. The pullout test can be properly modelled by the proposed formulation herein. The numerical results demonstrate the accuracy and robustness of the proposed formulation.

2 Nonlinear 1DBEM/BEM coupling formulation

2.1 3D BEM singular formulation

The BEM displacements integral equation represents the solid (Ω) mechanical behaviour. This equation can be obtained through the weighted residual technique as presented by Brebbia [4] and it is written as follows:

$$c_{ij}(\mathbf{x}^s)u_j(\mathbf{x}^s) + \int_\Gamma T^*_{ij}u_j(\mathbf{x}^f)d\Gamma = \int_\Gamma U^*_{ij}p_j(\mathbf{x}^f)d\Gamma + \int_\Omega U^*_{ki}b_i d\Omega \tag{1}$$

in which u_i and p_i represent displacements and tractions at the boundary, respectively. Γ is the boundary of Ω. c_{ij} is the free term, which is equal to the Kronecker delta (δ_{ij}) for internal points and $0.5\delta_{ij}$ for points at smooth boundaries. U^*_{ij} and T^*_{ij} are the Kelvin's fundamental solutions, found in Brebbia and Dominguez [5], for displacements and tractions, respectively.

The BEM solves Eq. 1 in approximate form. Then, the geometry and mechanical fields are approximated by Lagrangian isoparametric elements positioned at the boundary (Γ). Linear quadrilateral elements with 4 fodes are utilised herein. Besides, non-smooth geometries and discontinuous boundary conditions can be handled through discontinuous and semi-continuous boundary elements. Equation. 1 must be evaluated for all collocation points (source points) to represent the solid's mechanical behaviour. Because of the singular nature of the fundamental solutions, singularity subtraction technique is applied herein, as presented in Guiggiani et al. [6]. Otherwise, the regular kernels are numerically integrated by Gauss-Legendre scheme. Hence, Eq. 1 can be algebraically written as follows:

$$\mathbf{Hu} = \mathbf{Gp} + \int_\Omega U^*_{ki}b_i d\Omega \tag{2}$$

where the matrices $\mathbf{H}$ and $\mathbf{G}$ contain, respectively, the integration of kernels T^*_{ij} and U^*_{ij} along Γ. The domain term has not been treated so far, thus it cannot be written in a algebraic form. This term will be numerically treated in the coupling formulation section.

Equation 1 can also be used to represent internal points' displacements. This expression is algebraically written as follows:

$$\mathbf{u_i} + \mathbf{Hu} = \mathbf{Gp} + \int_\Omega U^*_{ki}b_i d\Omega \tag{3}$$

where u_i is the vector of displacements of the internal point i.

2.2 1DBEM in space: reinforcements modelling

The 1DBEM displacements integral equation can also be obtained through the weighted residual technique applied for 1D domains ($\bar{x}$) as described by Rodrigues Neto and Leonel [2] and it is written as follows:

$$u_i - N^*_{i1}u_1 + N^*_{in}u_n = -u^*_{i1}N_1 + u^*_{in}N_n + \int_0^L \phi_j(\bar{x})\, u^*_{i\bar{x}}\, d\bar{x}\; p_j \tag{4}$$

in which subscripts 1 and n represent the 1D domain endpoints. u_i and N_i are, respectively, the axial displacement and internal force at the i point. ϕ_j are the Lagrangian functions used for the distribuited load approximation over the domain $\bar{x}$, using its nodal values p_i. u^*_{ij} and N^*_{ij} are the fundamental solutions for axial displacements and internal forces, respectively, which can be found in Banerjee and Butterfield [7], Antes [8].

The integral formulation (Eq. 4) requires the discretisation of the structural boundaries into parametric elements. One notices that the boundary is composed only of the 1D element endpoints, i.e., $i = 1$ and $i = n$. Any other value for i leads to an internal point equation. However, internal points must be accounted in the 1DBEM algebraic system, to improve the accuracy of the distributed load representation. Hence, the 1DBEM formulation enables high-order isoparametric elements. Thus, after applying the element's approximations, Eq. 4 can be algebraically written as follows:

$$\bar{\mathbf{H}}\mathbf{u} = \bar{\mathbf{G}}\mathbf{n} + \bar{\bar{\mathbf{G}}}\mathbf{p} \tag{5}$$

where $\bar{\mathbf{H}}$ and $\bar{\mathbf{G}}$ contain the values of the fundamental solutions N^*_{sf} and u^*_{sf}, respectively, applied in the boundary points. $\mathbf{u}$, $\mathbf{p}$ and $\mathbf{n}$ vectors contain, respectively, the nodal values of axial displacement, nodal values of distributed force and concentrated loads. This expression is so far valid for the local coordinate system. The following global expression can be written by applying axial rotation as described by Kassimali [9] and considering $\mathbf{n} = \mathbf{0}$:

$$\mathbf{K_F u_F} = \mathbf{G_F p_F} \tag{6}$$

in which $\mathbf{u_F}$ and $\mathbf{p_F}$ vectors contain the values of $\mathbf{u}$ and $\mathbf{p}$ in the global coordinate system.

2.3 Algebraic equations of the coupling formulation

Consider the reinforcements completely embedded into a solid Ω and positioned along the line $\bar{\Gamma}$. The coupling scheme accounts for the mechanical interaction among reinforcements and domain, which is represented by the adherence force.

The adherence force is modelled as one-dimensional distributed load along the reinforcement's line $\bar{\Gamma}$. However, one-dimensional loads applied in a three dimensional domain lead to divergent singular values in the fundamental solutions, i.e., which cannot be regularised. Thus, a matching approximation is required, which is similar to the "special element" proposed for FEM/BEM couplings in Coda et al. [10]. The adherence force in Ω is assumed to be applied over a two-dimensional surface, which represents the external surface area of the reinforcements. A cylindrical shell of radius R_F is adopted herein. Considering the reinforcements as thin elements, i.e., with a length higher than R_F, one can writes the following simplification:

$$\mathbf{p_D} = 2\pi R_F \mathbf{Q_i} \tag{7}$$

where $\mathbf{Q_i}$ is the value of the distribuited force over the cylindrical shell, assumed as constant along the angular direction θ. Thus, the integration of the adherence force over the reinforcements elements can be accounted in the domain integration of Eq. 1 and numerically evaluated as follows:

$$\begin{aligned}&\int_{\bar{\Gamma}} U^*_{ij}(\mathbf{p_D})_j d\Gamma = \\ &\sum_{g_1=1}^{np_1}\left[\sum_{g_2=1}^{np_2}\left[U_{ij}\left(\mathbf{x}^f(\xi_{g_1},\xi_{g_2}),\mathbf{x}^s\right)|\mathbf{jac_2}(\xi_{g_2})|\,\omega_{g_2}\right]|\mathbf{jac_1}(\xi_{g_1})|\,\omega_{g_1}\phi_m(\xi_{g_1})\right]\frac{(\mathbf{p_D})_j}{2\pi R_F}\end{aligned} \tag{8}$$

where g_1 and g_2 represent the numerical integrations used for the axial coordinate ($\bar{x}$) and the angular coordinate (θ), respectively. ξ_i, ω_{g_i} and np_i are the dimensionless coordinates, weight values and total number of integration points of the numerical integration i, respectively.

Figure 1 illustrates scheme of this special integration over a reinforcement element considering a source point positioned at $\bar{\Gamma}$, $np_2 = 4$ and a fixed coordinate ξ_{g_1}.

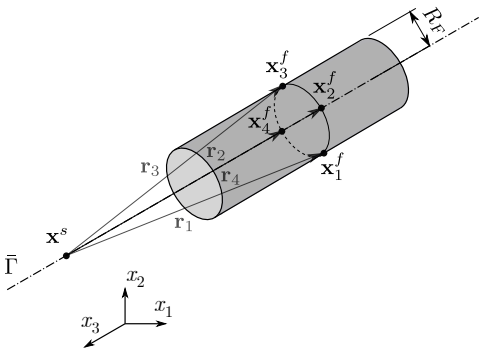

Figure 1. Integration scheme over a reinforcement element, considering 4 integration points over the angular coordinate and a fixed axial coordinate.

Therefore, the adherence force can be properly accounted as a body force into the BEM formulation through Eq. 8. Hence, the BEM integral equation for boundary points (Eq. 2) can be rewritten as follows:

$$\mathbf{H_{CC}u_C} = \mathbf{G_{CC}p_C} + \mathbf{G_{CF}p_D} \tag{9}$$

where the term $\mathbf{G_{CF}p_D}$ is the particular form of the domain term obtained by applying Eq. 8. The subscripts $\mathbf{C}$ and $\mathbf{F}$ indicate boundary and fibre, respectively. The subscript $\mathbf{D}$ indicates the internal point of Ω coincident with a fibre point. In the above equation, a matrix $\mathbf{H_{XY}}$ or $\mathbf{G_{XY}}$ result from source point at $\mathbf{X}$ and field point at $\mathbf{Y}$.

The BEM integral equation for internal points (Eq. 3) can also be rewritten herein. This equation must be applied for internal points coincident with the reinforcements nodes, i.e., $\mathbf{u_i} = \mathbf{u_D}$. Thus:

$$\mathbf{u_D} = \mathbf{G_{FC}p_C} - \mathbf{H_{FC}u_C} + \mathbf{G_{FF}p_D} \tag{10}$$

2.4 Algebraic representation of the coupling formulation considering bond-slip effects

The nonlinear bond-slip formulation accounts for the relative displacement among reinforcement and matrix. Therefore, the compatibility of displacements is written as follows:

$$\mathbf{s} = \mathbf{u_D} - \mathbf{u_F} \tag{11}$$

where $\mathbf{s}$ is the vector of nodal slip.

The energy dissipation phenomenon during the slipping process is represented by the adherence law, which relates slip and adherence forces. With that, one can determine the variables values for an equilibrium configuration. Figure 2 illustrates the adherence law adopted herein. This is a multi-linear function inspired by the most often suggested laws in the simulation of reinforced concrete, CEB-FIP [11], Huang et al. [12].

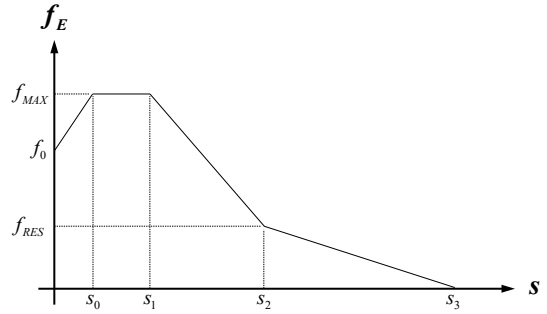

(a) Graphic representation

$$\begin{aligned}
f(s) &\le f_0 && , \quad s = 0 \\
f(s) &= f_0 + \left(\tfrac{f_{MAX}-f_0}{s_0}\right) s && , \quad 0 < s \le s_0 \\
f(s) &= f_{MAX} && , \quad s_0 < s \le s_1 \\
f(s) &= f_{MAX} - \left(\tfrac{f_{MAX}-f_{RES}}{s_2-s_1}\right)(s - s_1) && , \quad s_1 < s \le s_2 \\
f(s) &= f_{RES} - f_{RES}\left(\tfrac{s-s_2}{s_3-s_2}\right) && , \quad s_2 < s \le s_3
\end{aligned}$$

(b) Mathematical representation

Figure 2. Bond-slip behaviour modelling.

In order to properly simulates the pull-out test, the formulation must allow for boundary conditions applied directly at the reinforcing bar outside Ω. Thus, a connection element proposed in Rodrigues Neto and Leonel [2] is used herein, as illustrated in Fig. 3. This approach adds extra nodes in the reinforcements mesh, in which the prescribed displacement $\bar{\mathbf{u}}_\mathbf{D}$ is applied.

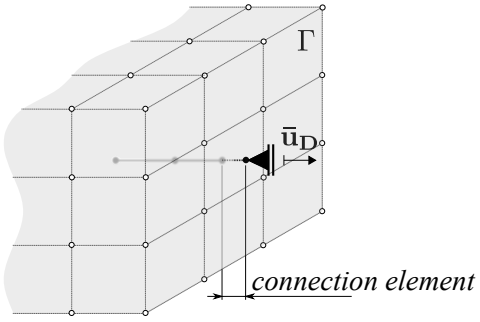

Figure 3. Prescribed displacement at reinforcements using the connection element.

Therefore, Eq. 6 is updated by Eq. 11 and the consideration of the connection element with the applied $\bar{\mathbf{u}}_\mathbf{D}$. Thus:

$$\mathbf{K_F u_D} + \bar{\bar{\mathbf{K}}}_{\text{sup}}\bar{\mathbf{u}}_\mathbf{D} + \mathbf{G_E f_D} = \mathbf{K_F s} \tag{12a}$$

$$\bar{\bar{\mathbf{K}}}_{\text{inf}}\mathbf{u_D} + \bar{\bar{\mathbf{K}}}_{\text{diag}}\bar{\mathbf{u}}_\mathbf{D} + \bar{\bar{\mathbf{G}}}_{\text{inf}}\mathbf{f_D} = \mathbf{f}_{\text{reac}} + \bar{\bar{\mathbf{K}}}_{\text{inf}}\mathbf{s} \tag{12b}$$

where $\mathbf{f}_{\text{reac}}$ is the reaction force associated with the prescribed displacement $\bar{\mathbf{u}}_\mathbf{D}$. All adherence forces are nil at the connection element nodes, since their position is outside the domain Ω. The matrices $\mathbf{K_F}$ and $\mathbf{G_F}$ are the original terms of the reinforcements matrices. Besides, $\bar{\bar{\mathbf{K}}}_\mathbf{inf}$, $\bar{\bar{\mathbf{K}}}_\mathbf{sup}$, $\bar{\bar{\mathbf{K}}}_\mathbf{diag}$, $\bar{\bar{\mathbf{G}}}_\mathbf{inf}$, $\bar{\bar{\mathbf{G}}}_\mathbf{sup}$ and $\bar{\bar{\mathbf{G}}}_\mathbf{diag}$ are the extra terms obtained by the consideration of the connection element nodes in addition to the original reinforcements mesh. Equation. 12a represents the nodal equilibrium of the original reinforcement mesh and Eq. 12b represents the equilibrium of the connection element nodes.

The algebraic system of equations for the coupling formulation is obtained by considering Eq. 9, Eq. 10 and Eq. 12. Then:

$$\begin{bmatrix} \mathbf{A_{CC}} & \mathbf{0} & -\mathbf{G_{CF}} & \mathbf{0} \\ \mathbf{B_{FC}} & \mathbf{I} & -\mathbf{G_{FF}} & \mathbf{0} \\ \mathbf{0} & \mathbf{K_F} & \mathbf{G_F} & \mathbf{0} \\ \mathbf{0} & \bar{\bar{\mathbf{K}}}_{\text{inf}} & \bar{\bar{\mathbf{G}}}_{\text{inf}} & -\mathbf{I} \end{bmatrix} \begin{Bmatrix} \mathbf{x_C} \\ \mathbf{u_D} \\ \mathbf{p_D} \\ \mathbf{f}_{\text{reac}} \end{Bmatrix} = \begin{bmatrix} \bar{\mathbf{A}}_{\mathbf{CC}} \\ \bar{\mathbf{B}}_{\mathbf{FC}} \\ \mathbf{0} \\ \mathbf{0} \end{bmatrix} \{\tilde{\mathbf{p}}_{\mathbf{C}}\} + \begin{bmatrix} \mathbf{0} \\ \mathbf{0} \\ -\bar{\bar{\mathbf{K}}}_{\text{sup}} \\ -\bar{\bar{\mathbf{K}}}_{\text{diag}} \end{bmatrix} \{\bar{\mathbf{u}}_{\mathbf{D}}\} + \begin{bmatrix} \mathbf{0} \\ \mathbf{0} \\ \mathbf{K_F} \\ \bar{\bar{\mathbf{K}}}_{\text{inf}} \end{bmatrix} \{\mathbf{s}\} \tag{13}$$

The nonlinear problem is solved through the Newton-Raphson technique, which consistis of trial and correction phases. Firstly, the prescribed boundary conditions are sub-divided into load steps: $\mathbf{\Delta \tilde{p}_C}$ and $\mathbf{\Delta \bar{u}_D}$. The trial phase consists of assuming the slip variation $\mathbf{\Delta s}$ as nil and apply the loads ($\mathbf{\Delta \tilde{p}_C}$ and $\mathbf{\Delta \bar{u}_D}$) into Eq. 13. The obtained adherence forces are evaluated in the adherence law (Figure 2(b)) accounting for the accumulated $\mathbf{s}$ response as follows:

$$\mathbf{\Delta p_{des}} = -\mathbf{p_D} + \mathbf{\Delta p_E} - \mathbf{p_{ADM}} \tag{14}$$

where $\mathbf{p_{ADM}}$ are the admissible values provided by the adherence law and $\mathbf{p_{des}}$ is the unbalanced forces vector.

The correction phase identifies the k nodes in which $\mathbf{\Delta p}^k_{\mathbf{des}} \neq 0$. Then, these unbalanced values are reapplied into the system as follows:

$$\begin{bmatrix} \mathbf{A_{CC}} & \mathbf{0} & \mathbf{0}^k & -\mathbf{G}^j_{\mathbf{CF}} & \mathbf{0} \\ \mathbf{B_{FC}} & \mathbf{I} & \mathbf{0}^k & -\mathbf{G}^j_{\mathbf{FF}} & \mathbf{0} \\ \mathbf{0} & \mathbf{K_F} & -\mathbf{K}^k_{\mathbf{F}} & \mathbf{G}^j_{\mathbf{F}} & \mathbf{0} \\ \mathbf{0} & \bar{\bar{\mathbf{K}}}_{\text{inf}} & -\bar{\bar{\mathbf{K}}}^k_{\text{inf}} & \bar{\bar{\mathbf{G}}}^j_{\text{inf}} & -\mathbf{I} \end{bmatrix} \begin{Bmatrix} \delta\mathbf{x_C} \\ \delta\mathbf{u_D} \\ \delta\mathbf{s}^k \\ \delta\mathbf{p}^j_{\mathbf{D}} \\ \delta\mathbf{p}_{\text{reac}} \end{Bmatrix} = \begin{bmatrix} \mathbf{G}^k_{\mathbf{CF}} \\ \mathbf{G}^k_{\mathbf{FF}} \\ -\mathbf{G}^k_{\mathbf{F}} \\ -\bar{\bar{\mathbf{G}}}^k_{\text{inf}} \end{bmatrix} \left\{ \mathbf{\Delta p}^k_{\mathbf{des}} \right\} \tag{15}$$

Then, the variables $\mathbf{\Delta x_C}$, $\mathbf{\Delta u_D}$, $\mathbf{\Delta s}$ and $\mathbf{\Delta p_D}$ are accumulated by its variation values (δ). The convergence verification consists of evaluating the modulus of $\mathbf{\Delta p_{des}}$ normalised by the accumulated values $\mathbf{p_D}$.

3 Numerical application: the pullout test

The pullout test consists of a steel bar immersed into a concrete cylinder as illustrated in Fig. 4(a). The steel bar is pulled-out from its left extremity. Experimental results of this test have been presented by Zulini [13] and are used herein as reference.

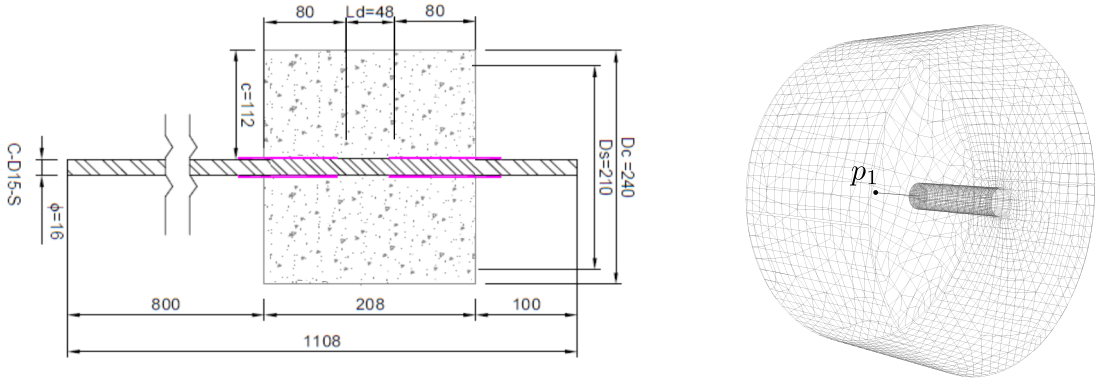

(a) (b)

Figure 4. Fibre pull-out test in reinforced concrete: specimen's scheme in mm (a) , Zulini [13], adapted, and BEM mesh for the numerical analysis (b).

Figure 4(b) illustrates the BEM mesh for the numerical analysis, which is composed of 3816 linear quadrilateral elements and 4271 collocation points. 100 quadratic reinforcement elements discretise the steel bar. Previous analysis have shown mesh convergence for this model. Zulini [13] provides experimental data regarding the relative displacement of the steel bar right end versus the normalised adherence stress (τ_{ad}). This relative displacement is numerically represented by the slip value at the point p_1 illustrated in Fig.4(b). τ_{ad} is evaluated from the reaction force $\mathbf{f}_{\text{reac}}$ at the opposite fibre extremity, as follows:

$$\tau_{\text{ad}} = \frac{\mathbf{f}_{\text{reac}}/\pi\phi l_b}{(70/f_{cm})^{1/4}} \tag{16}$$

where ϕ is the steel rebar diameter, l_b is the length of the adherence region and f_{cm} is the concrete compression strength.

The following mechanical properties are considered herein: concrete Young modulus and Poisson ratio equal to 41.16 GPa and 0.2, respectively; $f_{cm} = 67.44$ MPa; Young modulus of the steel bar equals to 201.8 GPa and $\phi = 16$ mm. The prescribed displacement at the steel rebar end ($\bar{\mathbf{u}}_{\mathbf{D}} = 10$ mm) represents the action of the pullout claw machine. The adherence law considers the following parameters, based on the suggested values from Huang et al. [12]: $s_0 = 0.8$ mm; $s_1 = 2.0$ mm; $s_2 = 10.0$ mm; $s_3 = 3\,s_2$; $f_{MAX} = 0.55\,(f_{cm}\pi\phi)$; $f_{RES} = 0.4 f_{MAX}$. The nonlinear process for the bond-slip analysis has been solved by 150 load steps and tolerance for convergence of 10^{-9}. The iterative process required the amount of iterations in the range of 1 to 15 for convergence within each load step.

Figure 5 illustrates the results of the proposed model ("Multi-linear law") and the reference responses ("Experimental"). Besides, an alternative law ("Linear law") is illustrated herein. This law accounts for the same parameters previously mentioned and assumes $s_0 = 0$. This figure demonstrates the excellent agreement among the numerical and experimental responses for all slip values. The numerical approach accurately predicted the expected behaviour. The proposed multi-linear law leads to more accurate results, since it is closer to experimental laws often suggested for this application.

Figure 5. Adherence stress as function of the slip at point p_1.

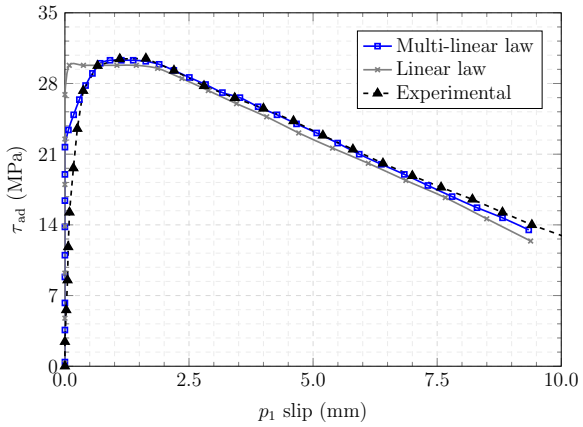

Figure 6 illustrates the nodal displacements at the boundary, along directions x and z, at the last load step. Reinforcements and boundary meshes are illustrated herein. Figure 6 presents a consistent behaviour for displacements along the boundary and one can clearly see the steel bar being pulled out of the concrete specimen. Moreover, the proposed coupling procedure leads to the accurate stress transfer among the structural elements involved in system. Such behaviour has major importance during the nonlinear process. Besides, Fig. 6(b) shows clearly the symmetrical response obtained around the cylinder's central axis, which is within the expected behaviour.

4 Conclusions

The nonlinear 1DBEM/BEM coupled formulation for the mechanical analysis of 3D reinforced structures and materials was successfully presented in this study. The numerical application demonstrate its robustness and accuracy in modelling complex 3D engineering problems, such as the pullout test. Particularly, the accuracy on the maximum adherence stress value and the post-peak behaviour must be emphasised. It is worth stressing the real 3D aspect of this modelling. Besides, the analysis of the bond-slip effects via 3D BEM formulations is original in the literature. The efficiency of the formulation was also illustrated, regarding the reduced number of degrees of freedom in the model and the reduced number of iterations to achieve convergence. Therefore, the proposed formulation is robust, stable and has large potential for solving complex real-life structural problems.

Acknowledgements. Sponsorship of this research project by the São Paulo State Foundation for Research (FAPESP), project number 2018/20253-4, is greatly appreciated.

Figure 6. Boundary nodal displacements in directions x (a) and z (b).

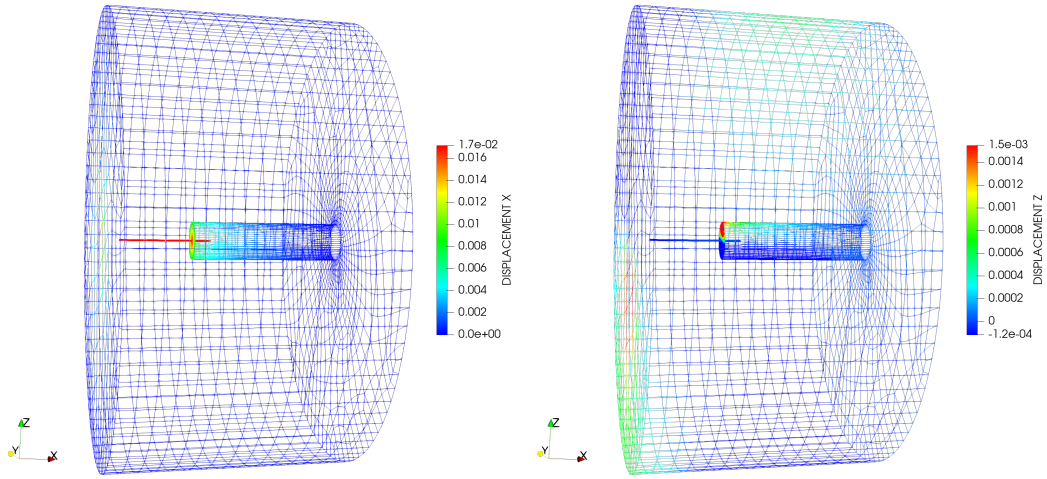

(a) (b)

Authorship statement. The authors hereby confirm that they are the sole liable persons responsible for the authorship of this work, and that all material that has been herein included as part of the present paper is either the property (and authorship) of the authors, or has the permission of the owners to be included here.

References

[1] Zienkiewicz, O., Kelly, D., & Bettess, P., 1977. The coupling of the finite element method and boundary solution procedures. *International journal for numerical methods in engineering*, vol. 11, n. 2, pp. 355–375.

[2] Rodrigues Neto, A. & Leonel, E. D., 2019. The mechanical modelling of nonhomogeneous reinforced structural systems by a coupled BEM formulation. *Engineering Analysis with Boundary Elements*, vol. 109, pp. 1 – 18.

[3] Rocha, F. C., Venturini, W. S., & Coda, H. B., 2014. Sliding frame-solid interaction using BEM/FEM coupling. *Latin American Journal of Solids and Structures*, vol. 11, pp. 1376 – 1399.

[4] Brebbia, C. A., 1978. Weighted residual classification of approximate methods. *Applied Mathematical Modelling*, vol. 2, n. 3, pp. 160 – 164.

[5] Brebbia, C. & Dominguez, J., 1994. *Boundary Elements: An Introductory Course*. Sydney Grammar School Press.

[6] Guiggiani, M., Krishnasamy, G., Rudolphi, T. J., & Rizzo, F. J., 1992. A General Algorithm for the Numerical Solution of Hypersingular Boundary Integral Equations. *Journal of Applied Mechanics*, vol. 59, n. 3, pp. 604–614.

[7] Banerjee, P. K. & Butterfield, R., 1981. *Boundary element methods in engineering science*, volume 17. McGraw-Hill, London.

[8] Antes, H., 2003. Fundamental solution and integral equations for timoshenko beams. *Computers & structures*, vol. 81, n. 6, pp. 383–396.

[9] Kassimali, A., 2012. *Matrix Analysis of Structures*. Cengage Learning, Stamford, 2 edition.

[10] Coda, H. B., Venturini, W. S., & Aliabadi, M. H., 1999. A general 3D BEM/FEM coupling applied to elastodynamic continua/frame structures interaction analysis. *International Journal for Numerical Methods in Engineering*, vol. 46, n. 5, pp. 695–712.

[11] CEB-FIP, 1990. Bulletin d'information n. 195/197. *Comité Euro-International du Béton - FIP Model Code*, vol. 1.

[12] Huang, Z., Engström, B., & Magnusson, J., 1996. Experimental investigation of the bond and anchorage behaviour of deformed bars in high strength concrete. *Chalmers University of Technology, Division of Concrete Structures, Report*, vol. 95, n. 4, pp. 32.

[13] Zulini, I., 2019. Effects of confinement in bond between reinforcement bar and high strength concrete. Master's thesis, Department of Structural Engineering, São Carlos School of Engineering, University of São Paulo, São Carlos.